DETECTION OF CRESCENT SAND DUNES CONTOURS IN SATELLITE IMAGES USING AN ACTIVE SHAPE MODEL WITH A CASCADE CLASSIFIER

M. A. Azzaoui [a,*], M. Adnani [a], H. El Belrhiti [b], I. E. Chaouki [c], L. Masmoudi [a]

[a] Laboratoire d'Electronique et de Traitement du Signal/ Géomatique (LETS/Géomat Faculté des Sciences de Rabat, Université Mohammed V-Agdal, 4 Avenue Ibn Battouta B.P. 1014 RP, Rabat, Maroc. - azzaoui.m.amine@gmail.com, adnani.manar@gmail.com, lhmasmoudi@gmail.com

[b] Département des Sciences Fondamentales et Appliquées. Institut Agronomique et Vétérinaire Hassan II. BP 6202, 10101 – Rabat, Maroc - helbelrhiti@gmail.com or h.elbelrhiti@iav.ac.ma

[c] Ecole Nationale des Sciences Appliquées d'Agadir, Maroc. B.P. 1136. - b.chaouki@uiz.ac.ma

WG VII/4 - Methods for Image Classification – Full Papers

KEY WORDS: Remote Sensing, IKONOS, High resolution satellite images, Cascade classifiers, Active Shape Model, Local Binary Patterns, Haar features, SURF, SVM, barchans dunes, desertification

ABSTRACT:

Crescent sand dunes called barchans are the fastest moving sand dunes in the desert, causing disturbance for infrastructure and threatening human settlements. Their study is of great interest for urban planners and geologists interested in desertification (Hugenholtz et al., 2012). In order to study them at a large scale, the use of remote sensing is necessary. Indeed, barchans can be part of barchan fields which can be composed of thousands of dunes (Elbelrhiti et al.2008). Our region of interest is located in the south of Morocco, near the city of Laayoune, where barchans are stretching over a 400 km corridor of sand dunes.

We used image processing techniques based on machine learning approaches to detect both the location and the outlines of barchan dunes. The process we developed combined two main parts: The first one consists of the detection of crescent shaped dunes in satellite images using a supervised learning method and the second one is the mapping of barchans contours (windward, brink and leeward) defining their 2D pattern.

For the detection, we started by image enhancement techniques using contrast adjustment by histogram equalization along with noise reduction filters. We then used a supervised learning method: We annotated the samples and trained a hierarchical cascade classifier that we tested with both Haar and LBP features (Viola et Jones, 2001; Liao et al., 2007). Then, we merged positive bounding boxes exceeding a defined overlapping ratio. The positive examples were then qualified to the second part of our approach, where the exact contours were mapped using an image processing algorithm: We trained an ASM (Active Shape Model) (Cootes et al., 1995) to recognize the contours of barchans. We started by selecting a sample with 100 barchan dunes with 30 landmarks (10 landmarks for each one of the 3 outlines). We then aligned the shapes using Procrustes analysis, before proceeding to reduce the dimensionality using PCA. Finally, we tested different descriptors for the profiles matching: HOG features were used to construct a multivariate Gaussian model, and then SURF descriptors were fed an SVM. The result was a recursive model that successfully mapped the contours of barchans dunes.

We experimented with IKONOS high resolution satellite images. The use of IKONOS high resolution satellite images proved useful not only to have a good accuracy, but also allowed to map the contours of barchans sand dunes with a high precision. Overall, the execution time of the combined methods was very satisfying.

1. INTRODUCTION

1.1 Sand dunes remote sensing

Remote sensing has been used by earth science scientists to study Aeolian sand dunes. It started from the 70s (Breed and Grow, 1979), where scientists showed the existence of sand dunes on Mars (Cutts and Smith,1973) and Venus (Florensky et al.,1977) and started studying the organization of groups of sand dunes. The seminal work of (McKee, 1979) relied on RS for the taxonomy and the mapping of dunes. It allowed exploring the influence of controlling parameters such as the wind patterns, the type of vegetation and the availability of sand on the terrain (Wasson and Hyde, 1983). While studies in the 80s focused on individual dunes, the important progress of computer science that took place in the 90s induced the interest of scientists into the understanding of the reflectance of dune surfaces (Blumberg, 1998). In the 2000s, more advances were made in the quantitative aspects of dunes morphology and dynamics (Vermeesch and Drake, 2008, Bishop 2010). The improvements of Remote Sensing spatial and spectral resolution also paved the way for new applications, such as the high resolution (LiDAR) used by (Wolfe and

Hugenholtz, 2009) to create a digital elevation model for identifying parabolic barchans dunes in Canada. Or the use of (ASTER) radiometric data used by (Scheidt et al. 2010) to create a mapping for the soil moisture in White Sands Dune field in New Mexico, USA. Also, the (HiRISE) camera on board of the Mars Reconnaissance Orbiter allowed more advanced researches on dunes morphology (Hansen et al., 2011, Azzaoui et al, 2016). The availability of geospatial datasets, from Corona, Landsat, MODIS, ASTER, HiRISE, MOC, MRO CTX, SRTM, ASTER GDEM, HiRISE DTM sometimes free, allowed more research to be conducted on the dynamics of barchans, which are usually located in remote areas (Sahara Desert, Namib Desert) or inaccessible areas, such as other planetary systems (Mars, Venus, Titan). The research in the latest years has been focusing on three main branches: the understanding of the activity of dunes, the description of dune patterns and hierarchies, and the discovery of extra-terrestrial dunes.

The dunes can be characterized by their potential of transporting sand. In fact, they form a continuum spanning from dunes that we can characterize as stabilized (do not show any change in their surface) and dunes that we can characterize as active (showing a loss or a gain of sand supply, which can be translated as an erosion or a deposition of sand). For instance, the 'star' dunes tend to accumulate as they are formed when there is a multi-directional wind with an important variability, while 'seif' dunes tend to form and extend under bidirectional winds. Conversely, 'barchan' dunes tend to migrate (Tsoar, 2001) as they are subject to unidirectional winds. Therefore, scientists emphasize the distinction between mobility and activity of sand dunes (Bullard et al. 1997), as dunes can be active without being necessary mobile. Also, dunes behaviour is described as depending on three interdependent factors: how much sand is available, how easy can it be moved by the wind, and what is the wind potential when moving it. Advances in remote sensing allowed scientists to track more effectively the quantitative morphodynamical changes of dunes activities. As a matter of fact, some scientists support the use of dunes systems as an indicator of climate change (Berger and Iams, 1996). Although dependent on climatic processes, other scientists showed that dunes systems are a complex non-linear physical system where lags can occur (Tsoar, 2005), which makes it difficult to use their activity as an indicator of climate change. Moreover, factors such as the vegetation, which is a primary impediment for any Aeolian sand transport (Buckley, 1987; Okin, 2008), can create sometimes a positive, and sometimes a negative feedback for the evolution of dunes activity, thus, adding more complexity to the system. Furthermore, some scientists consider it a better approach to study dunes as a biologic and a geomorphologic process (Hugenholtz and Wolfe, 2005).

1.2 Measuring sand dunes activity

Remote sensing has been used to measure the activity of dunes through three different means of evaluation: investigating what are the topographic changes, how much sand is available, and how does the dune shape changes.

Starting with topography, the use of shading can help evaluating the slope of bare sand dunes (Levin et al. 2004). Also, 3D models are suitable: The release of DEMs such as ASTER GDEM allowed more possibilities. As an example, (Hugenholtz and Barchyn 2010) proposed to calculate the EST (Equivalent Sand Thickness), which is the difference between the surface elevation and the base level elevation by smoothing to distinguish several layers of data. The LiDAR technology was also used to estimate topography of sand dunes (Reitz et al. 2010). The main advantage of topography is that it facilitates the computational simulation of fluid dynamics of wind (Jackson et al., 2011), which is the main source of energy that displaces the sand particles in arid and semi-arid regions.

Regarding the estimation of the availability of sand, historical data (including airborne imagery or maps) can be equally; if not more important than high resolution data as the temporal scale at which evolves the sand supply is determinant. With the increase of GIS software usage in the 90s, many hardcopies were digitized and the image parameters were corrected to allow reliable spatial measurements. (Anthonsen et al., 1996). One of the main challenges is the distinction between the open sand, the vegetation in the dunes, and the crust. In aerial photographs, it is relatively easy using contrast of brightness. With multispectral imagery, more detailed information was targeted such as the vegetation species and density, which can be influential for the sand activity. Near infrared can be used to distinguish vegetation types (Pinker and Karnieli 1995). Also, multispectral HRSI images allowed scientists to identify biological soil crust (Schatz et al., 2006). Biological soil crust can be made by many microphytes such as lichens, algae or bacteria which can reduce the sand available to be moved by wind (Tsoar and Karnieli, 1996).

For the dune shape change, it is one of the main indicators of the sand movement, though the quantitative models cannot be deducted straightforwardly. The majority of studies concerned with dunes shapes compare the 'nose to nose' distance between two temporal baseline images (Bailey and Bristow, 2004). But other indicators were used as well such as representing the dunes displacement with vectors (Levin et al., 2009, Jimenez et al., 1999), which is not always objective as it is difficult to determine the exact starting and ending points of sand dunes, and dunes don't have an invariable shape. Other researchers also used the area of the dune to produce better estimations (Levin and Ben-Dor, 2004). Besides, there are other approaches which fit polylines to each dune's ridges, then base their displacement calculation on the nose point and the two rear points (Bailey and Bristow, 2004). Other approaches generate the velocity field of dunes movement using image processing techniques (Necsoiu et al., 2009). Finally, many researches on the subject of the evolution of dunes shapes based their work on laboratory models (Durán et al., 2005; Hersen, 2005; Katsuki et al., 2011), which produces accurate and mathematically elegant models. However, they lacked field observations to validate them. Fortunately, the development of remote sensing approaches provided a way for experimental scientists to validate their mathematical models with an approximation of the field reality.

1.4 Structure of dunes

Allometric measures revealed linear correlation between dunes width and height (Andreotti et al., 2002). Also, the ratio between dunes width and the horn width is an indicator of whether the dunes are receiving more sand than they are losing through the horns (Hersen et al., 2004), or the opposite. Collectively, dunes organized in a complex field which can display specific patterns. Statistical approaches were used to quantify such patterns, for example the frequency and wavelength for the case of linear dunes (Bullard et al. 1995). Also, remote sensing was used to monitor the density modification (Al-Dabi et al. 1997). Simple models were used, such as using lines connecting dune crests to outline dunes spacing and orientation, and marking dunes breaking the pattern (Ewing et al. 2006). Other scientists were interested in dunes collision and dune to dune interaction (Ewing et al. 2010). Randomness in a sand dune field was also studied using nearest neighbor analysis (Wilkins and Ford 2007).

1.5 Dunes in other planetary systems

Many investigators worked on mapping dunes on Mars or Venus (Silvestro et al., 2010; Bourke et al., 2008; Ewing et al., 2010), but also on understanding their interaction with the wind. (Hayward et al. 2007) created a geospatial database with the centroids of dunes and the orientation of the slip faces, which were used as indicators of the prevailing wind direction. It is however difficult to confirm that the orientation is compatible with the present surface wind, as there are cases where morphological features indicate the past wind (Wolfe et al., 2004). Other studies based on remote sensing supposed that some shrinking dunes found in Mars are suggesting the existence of active saltation processes (Bourke et al. 2008). However, only digital terrain Models (DTM) could confirm such hypothesis.

1.6 Barchans dunes research objectives

As shown in the former chapter, many researchers centred their attention on understanding different sand dunes morphologies and dynamics from different perspectives.

In our research, we focus on barchans dunes, which are propagating crescent-shaped dunes that form under limited supply of sand, in roughly unidirectional winds (or current flow) and un-vegetated areas on firm, coherent basement (Elbelrhiti and Hargitai 2015). These factors made of barchans dunes, the fastest type of sand dunes, and as a result, they became a serious threat to human activities, mainly in arid or semi-arid areas, since they are continuously covering the roads, which not only raises the number of road accidents, but also isolates more such regions, and consequently limits their economic development. Moreover, the sand movement directly impacts exposed cities and villages, as it covers the local farm lands, and even houses, creating social tensions, and forcing the inhabitants to migrate. Therefore, decision makers, urban planners, and citizens need to be provided with useful and reliable information, to devise strategies to counter the progression of barchans dunes, mitigate their action, prevent their consequences, which requires to monitor their hazardous ramping. Our region of interest is located nearby Tarfaya city in the south of Morocco, which suffers from barchans dunes progression (Hersen 2005). Along with desertification concerns, some researchers also tend to study dunes systems as an indicator of climate change, or at least find correlations with climatic transformations. Finally, space explorers and geologists who try to understand geological systems of extra-terrestrial planetary landforms (Mars, Venus or Titan) are also interested by works related to sand dunes systems as they provide an insight towards a better grasp of the complexity of such environments.

1.7 Technical approaches for barchans detection

There are several problematics that arise when studying barchans dunes in high resolution satellite images. One of them is the vegetation which can be a discriminative attribute as we may use textural feature to discriminate bare dunes with the vegetated surroundings. However, when dunes have trailing sand, the textural attributes cannot reliably differentiate sand dunes with their surroundings. Another issue is the solar illumination which can result in an important effect on topography due to shadings. These artifacts can be exploited for the detection of barchans sand dunes as is the case in this work. Commensurability is another consideration for multi-temporal research works, as it is ensured by measuring a parameter in two or more different periods or seasons (especially regarding vegetation cover (Til et al. 2004). The final impediment of remote sensing is about matching field measurements with RS data. As an example (Nield and Baas, 2008) used growth curves to estimate the response of vegetation to topographical changes.

2. MATERIAL AND METHODS

2.1 Material

Our area of interest is located in the south of Morocco, in the Sahara Desert, between the cities of Tarfaya and Laayoune. It is worth noted that this region is distinguished by one of the longest barchans dunes corridors on Earth, spanning across 400 km, indicated in yellow in [Figure 1], courtesy of Sentinel Copernicus programme.
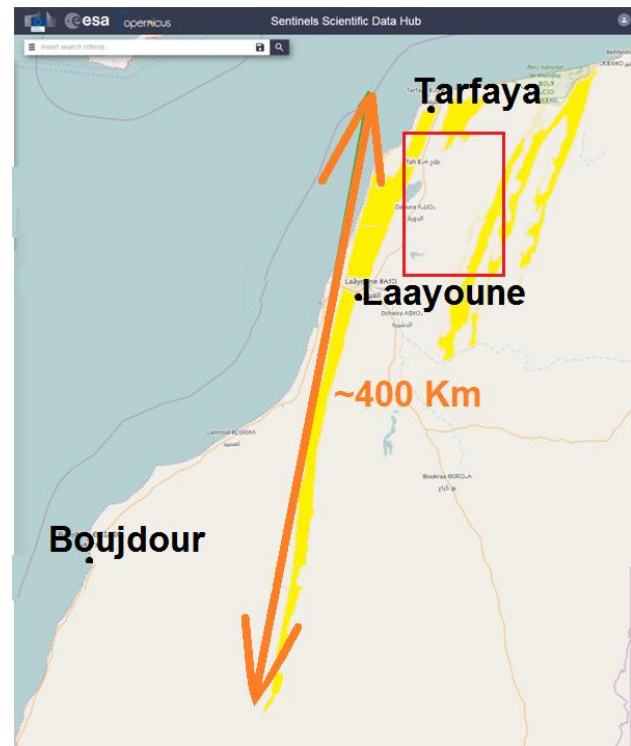

Figure 1: The study area location.
Yellow: Barchans corridor. Red box: Area of interest

Our goal is the segmentation of barchans dunes contours. Therefore, we used a high resolution satellite image in order to get an accurate outline of barchans of different sizes. The satellite image is from IKONOS, which includes include a 3.2m multispectral, and 0.82m panchromatic spatial resolution. It shows a field containing hundreds of barchans dunes. The following table contains the details about the image we used [Table.1].

Satellite	IKONOS
Location	South of Morocco, Sahara Desert
Coordinates	Between 27°26'8.6621"N, 13°08'5.2628"W and 27°41'1.0350"N, 13°22'0720"W
Scale	0.82m panchromatic
Date	July 23th, 2003
Area	~13 km²

Table 1. Image and location details

2.2 Methods

2.2.1 Process of detection, segmentation and morphology measurement: The approach we use is divided in three major stages: Detection of barchans dune, which takes in input a high resolution satellite image, runs computer vision and image processing algorithms and techniques, and produces as an output a set of barchans dunes candidates, which are surrounded by bounding boxes. The second stage is collecting the dunes candidates, and learning an active shape model which matches the contours of barchans (the windward, brink and leeward contours). The output is a collection of three splines, which constitutes a mathematical model for the 2D shape of a barchans dune. The third stage is a set of geometrical rules that we developed and applied on this simple model to generate a set of morphometric measures such as dunes width and horn width for which we explore basic statistical correlations.

2.2.2 Image enhancement and pre-processing: Multispectral images were scaled to the panchromatic image size, and then combined in an RGB manner, before being converted to a single channel grey scale image. Then, the resulting image was enhanced by applying first histogram equalization, then successively the Weiner filter and median filter, in order to reduce the noisiness.

2.2.3 Dataset preparation: As we use a machine learning approach and more specifically a supervised learning method, we started by annotating a learning dataset, through a program we developed specifically to map barchans dunes contours using spline curves. Once the annotation finished, we generated two sets of 65 positive and 65 negative images each, showing respectively barchans dunes and the surrounding environment (crust, vegetation, scattered sand or roads) [Figure 2].

2.2.4 Cascade classifier: To detect barchans dunes examples, we used a hierarchical cascade classifier (Viola et Jones, 2001; Liao et al., 2007), which we tested with two different descriptors: Haar and LBP. The cascade contained five stages with a false alarm rate of 5%. The cascade classifier used is based on a set of weak classifiers boosted to produce a vote on each stage of the hierarchy. Individually, a weak classifier is barely better than a coin flip, but when boosted they are a reliable model for decision-making.

2.2.5 Candidate fusion: After the execution of the learned model, we obtained a set of bounding boxes surrounding dunes candidates. The overlapping bounding boxes were merged into the maximum of their x,y coordinates. Moreover, the bounding box was enlarged by 20% to prepare for the next stage, which will require a buffer zone around the dunes candidates to operate.

2.2.6 Shapes alignment: The alignment of shapes is the first step in the second stage which is about training an ASM (Active shape Model) for segmenting barchans dunes contours. As each dune is identified with 30 landmarks: Each 10 landmarks correspond to a contour, which can be whether windward, brink or leeward. As barchans dunes have different scales and sizes, it is necessary to normalize their shapes. Therefore, we use a Procrustes Analysis, which is defined by an algorithm for which the goal is to minimize the distance of each shape from the mean of all shapes. It results into the minimization of scale, rotation and translation differences between shapes, using among others, the following transformation:

$$T_{X_t,Y_t,s,\theta} \begin{pmatrix} x \\ y \end{pmatrix} = \begin{pmatrix} X_t \\ Y_t \end{pmatrix} + \begin{pmatrix} s\cos\theta & -s\sin\theta \\ s\sin\theta & s\cos\theta \end{pmatrix} \begin{pmatrix} x \\ y \end{pmatrix}$$
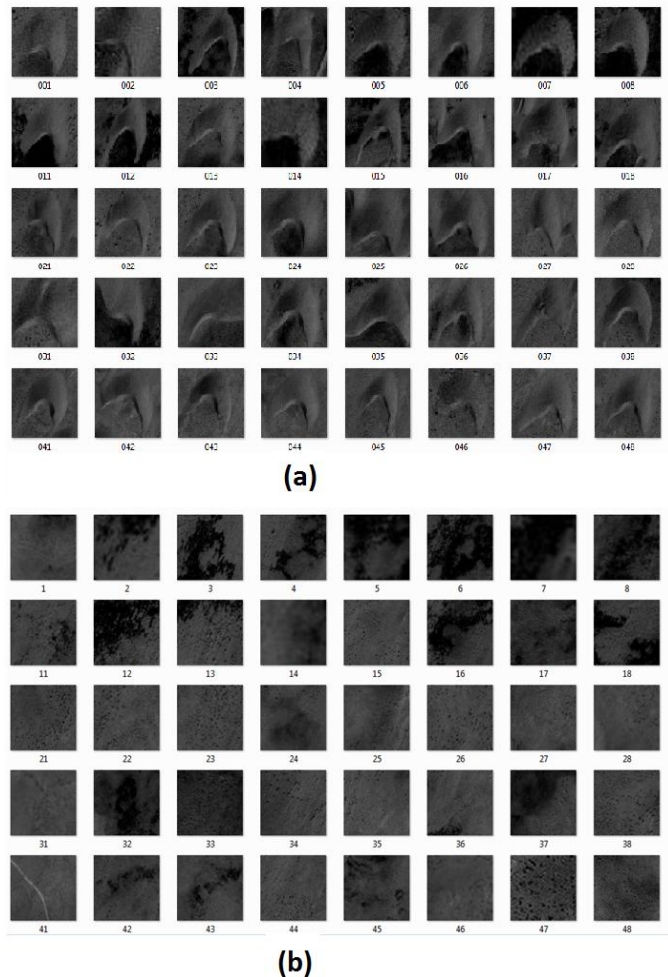

Figure 2: Dataset sample.
a: Positive examples of barchans dunes
b: Negative examples of surrounding terrain

2.2.7 Dimensionality reduction: As the model contains 30 landmarks, each dune is represented as 30 dimensional vector. We used a dimensionality reduction method PCA (Principal Component Analysis) to lower the number of parameters controlling the shape of a barchans dune. The reduced model was used to limit the variation of barchans shapes.

2.2.8 Profiles extraction: For each one of the 30 landmarks, a normal line was drawn, perpendicular to the corresponding outline of the barchans dune. Then from this profile, intensity derivatives were calculated. The combination of this intensity profiles allowed generating a multivariate Gaussian distribution model. This approach could be also slightly modified by using local feature descriptors such as SURF on and around each landmark, then use an SVM to learn to discriminate between the SURF points corresponding to the dune contour and the SURF points which are not falling in the contour of a barchans dune.

2.2.9 **Contours fitting:** In this step, we combine the former steps to detect the contour of a barchans dune. It starts by projecting the mean shape which is the result of shapes alignment and Procrustes analysis into the testing example. Then, we draw the normal of each landmark and extract the derivatives of intensity. Next, we moved each landmark independently along its normal, by minimizing the Mahalanobis distance between the model mean, and the possible other shapes.

$$f(\mathbf{g}_s) = (\mathbf{g}_s - \bar{\mathbf{g}})^T \mathbf{S}_g^{-1} (\mathbf{g}_s - \bar{\mathbf{g}})$$

Subsequently, a minimum is found, but to keep it on check an additional step is performed, which calls upon PCA learned model, and verifies that the shape found after Mahalanobis distance minimization is within predetermined boundaries of variance from the PCA mean model.

2.2.10 **Allometric features definition:** We defined a set of shape parameters summarized in [Figure 3]

w: Barchan dune width d_h: Horns distance

l : Barchan dune length C_w: Windward spline centroid

θ : Barchan dune direction C_b: Brink spline centroid

w_{h1}: First horn width C_l : Leeward spline centroid

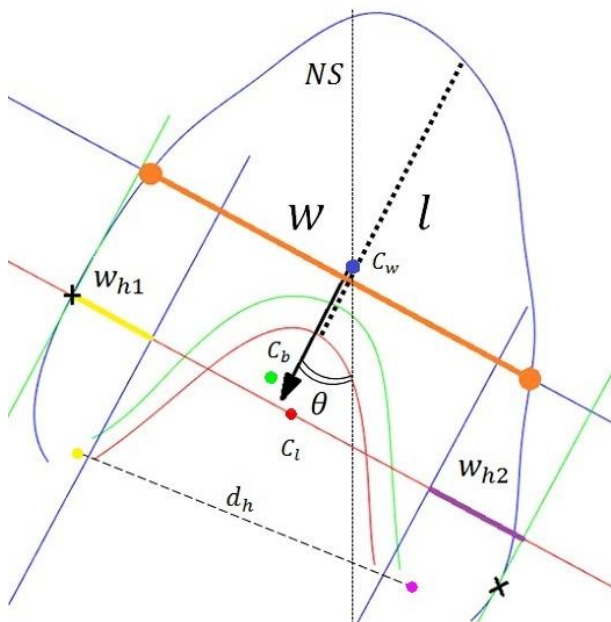w_{h2}: Second horn width   NS: North-South axis

Figure 3: 2D barchans dune allometric features

The barchans dunes were modeled by 3 spline curves. We calculated the centroids each of the three splines composing a barchan, and then we considered the direction of a barchan as aligned with the axis composed by windward spline centroid and the average of leeward and brink spline centroids. This orientation does not correspond necessary to the wind direction, and can only be indicative of the prevailing wind direction in specific cases. The width of a barchan was obtained by measuring the length of the segment fulfilling the following condition: It had to be the intersection between the dune direction orthogonal line passing by the crest and the windward spline. The barchan horns distance was measured between its first horn centroid and its second horn centroid. A horn centroid was simply defined as the barycenter of the corresponding ends of windward, brink and leeward splines. The horn width is the sum of the right and left horns widths. It was calculated by drawing a parallel line to the barchan direction and passing through the barycenter of leeward and brink splines ends. The second line was parallel to the barchan direction and passing through the first intersection with the windward spline, coming from outside towards the dune. The distance between those two lines approximated the horn width.

3. RESULTS

3.1 Dataset primary analysis

Following the primary collection of allometric results, we proceeded to a quantitative analysis summarized in [Table 2]:

	Mean	Standard deviation
Dunes direction (degree)	24.4917	8.8761
Dunes area (m²)	9611.5	7218.4
Dunes width (m)	96.7603	40.5764
Dunes width, horns-width ratio	2.9022	1.0217
Dunes spatial density(dune/km²)	11.7371	
Dunes covered area	0.1127 %	

Table 2. Statistical analysis of dunes features

Dune direction is not necessarily an indication the exact direction of movement of a barchans dune. However, it is related to prevailing wind direction, especially when we consider the mean dune direction. The dune area is the footprint of a dune and is calculated as the integral between dunes contours. Barchans mean width in our area of interest was 96m, with a standard deviation of 40m which classified them as medium to small barchans. The received sand flux is proportional to the barchans width, and the escaped sand flux is proportional to the width of its horns, therefore, the ration of these two parameters is an indicator of the shrinking or fattening of a barchans sand dune, thus providing an insight into its dynamics. The dune special density is a simple dune counting per square kilometre. The dunes covered area is sum of dunes area divided by the size of all the area of study.

3.2 Cascade classifier testing

The cascade classifier was used to detect barchans dunes of different scales. The Haar descriptor returned excellent detection results as it took advantage of the reflection of sun over the characteristic shape of barchans [Figure 4]
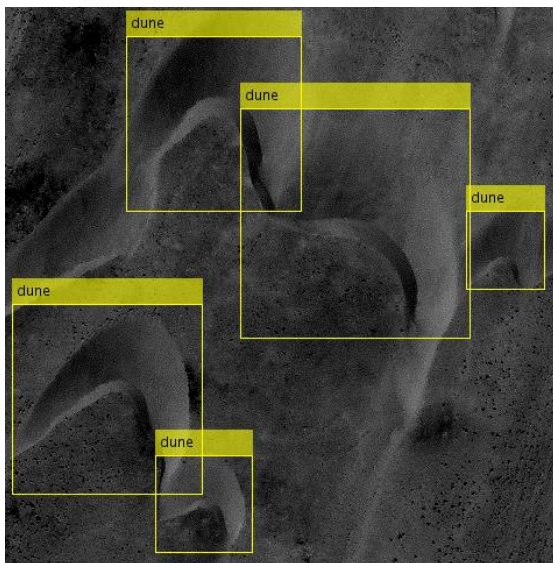
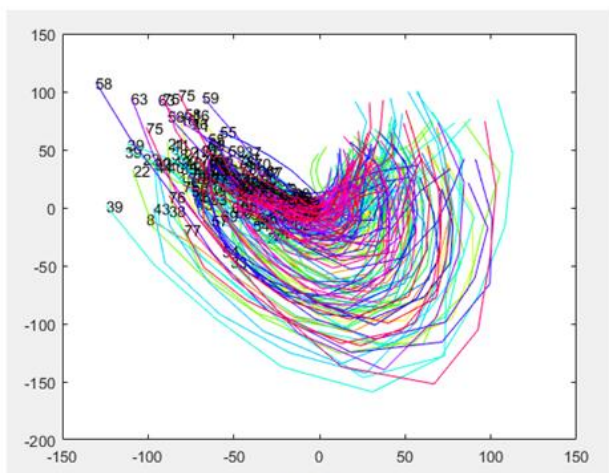Figure 4: Example of cascade classifier detection

3.3 Active shape model fitting:

(a)

(b)

Figure 5: a: Contours before alignment
b: Contours after Procrustes alignment

The shapes alignment was the first step, followed by applying PCA for dimensionality reduction [Table 3]

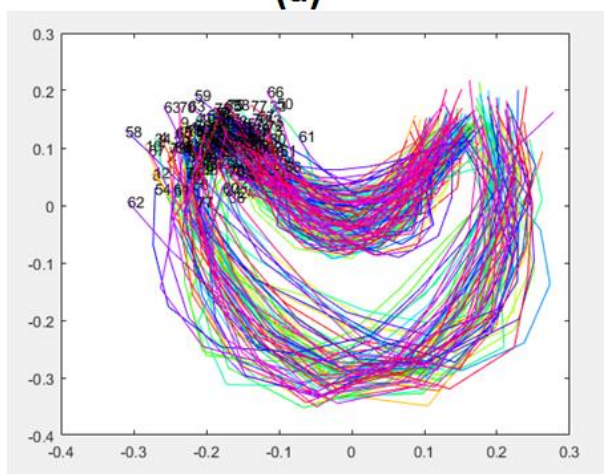|	Eigenvalues	Explained percentage
1	0.01455	32.56%
2	0.0088493	52.36%
3	0.0049935	63.54%
4	0.0038906	72.25%
5	0.0031457	79.29%
6	0.0018443	83.41%
7	0.0016682	87.15%
8	0.0012165	89.87%

Table 3: PCA Results

The modes of each barchans were constrained with a variance factor, to maintain the shape of dunes within a specific range [Figure 6], to insure a reasonable convergence [Figure 7].
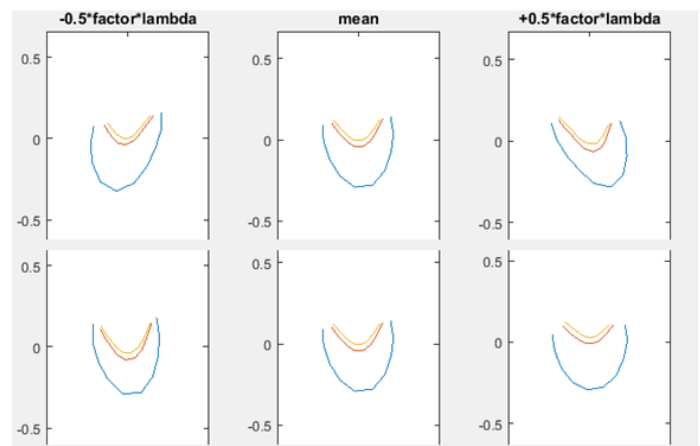

Figure 6: Example of 2 different modes with their mean in the central column, and adjacent, their respective variations
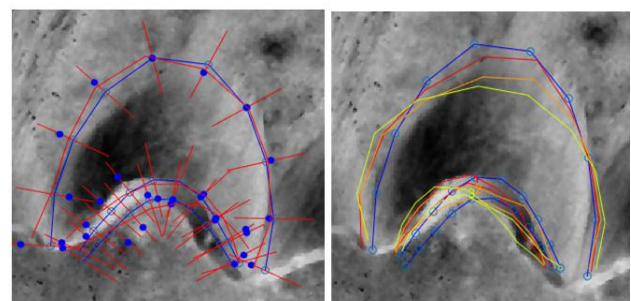

Figure 7: Left: Landmarks normal. Right: ASM convergence

3.4 Correlation of allometric measures

After few adjustments, we used our geometric model to collect allometric measures from barchans. Then, we explored the correlations between dunes width and height measurements [Figure 8], which is shown in the following equation:

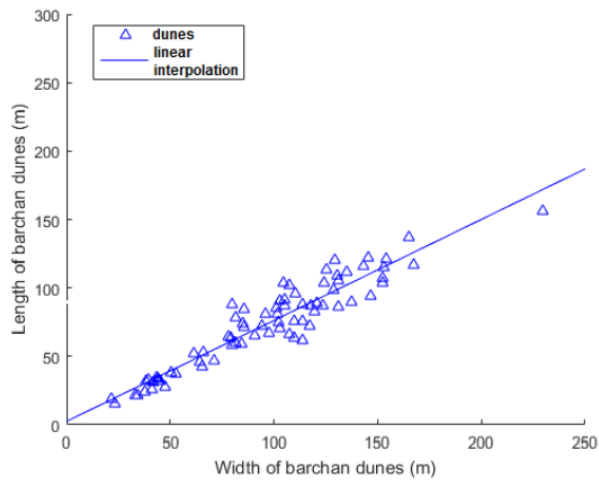$$l = 2.48 + 0.73 \times w : \|e\| = 91.2$$

Figure 8: Dunes length as function of dunes width

4. CONCLUSION

We proposed a process divided in three consecutive stages for the detection, segmentation and extraction of measures of barchans dunes. Our object based approach relied on machine learning and image processing. Indeed, the combination of a hierarchical detection algorithm, an active shape model for the segmentation of contours and a set of geometrical tools to extract dunes measures proves very useful, as we could found correlation between dunes features.

The method proposed can allow scientists to gather a large amount of data from thousands of dune automatically, using remote sensing, which can certainly provide a better insight into barchans dunes dynamics, for geologists, urban planners and decision makers who face desertification problems. Future works could extend the spatial and temporal scale.

REFERENCES

Al-Dabi, H., Koch, M., Al-Sarawi, M., El-Baz, F., 1997. Evolution of sand dune patterns in space and time in north-western Kuwait using Landsat images. Journal of Arid Environments 36, 15–24.

Andreotti, B. , Claudin, P., and Douady, S.: Selection of dune shapes and velocities part 1: Dynamics of sand, wind and barchans, Eur. Phys. J. B, 28, 321–339, 2002.

Anthonsen, K.L., Clemmensen, L.B., Jensen, J.H., 1996. Evolution of a dune from crescentic to parabolic form in response to short-term climatic changes: Råbjerg Mile, Skagen Odde, Denmark. Geomorphology 17, 63–77.

Azzaoui M.A, Adnani M. El Belrhiti H., Chaouki I.E., Masmoudi L. The International Archives of the Photogrammetry, Remote Sensing and Spatial Information Sciences, Volume XLI-B7, 2016 doi:10.5194/isprsarchives-XLI-B7-153-2016

Bailey, S.D., Bristow, C.S., 2004. Migration of parabolic dunes at Abberffraw, Anglesey, north Wales. Geomorphology 59, 165–174.

Berger, A.R., Iams, W.J., 1996. Geoindicators: Assessing Rapid Environmental Changes in Earth Systems. A.A. Balkema, Roterdam. 466 pp.

Bishop, M.A., 2010. Comparative nearest neighbor analysis of mega-barchanoid dunes, Ar Rub al Khali sand sea: the application of geographical indices to the understanding of dune field self-organization, maturity and environmental change. Geomorphology 120, 186–194.

Blumberg, D.G., 1998. Remote sensing of desert dune forms by polarimetric Synthetic Aperture Radar (SAR). Remote Sensing of Environment 65, 204–216.

Bourke, M.C., Edgett, K.S., Cantor, B.A., 2008. Recent aeolian dune change on Mars. Geomorphology 94, 247–255.

Breed, C.S., Grow, T., 1979. Morphology and distribution of dunes in sand seas observed by remote sensing. In: McKee, E.D. (Ed.), A Study of Global Sand Seas: U.S. Geological Survey Professional Paper, 1052, pp. 253–302.

Buckley, R., 1987. The effect of sparse vegetation cover on the transport of dune sand by wind. Nature 325, 426–428.

Bullard, J.E., Thomas, D.S.G., Livingstone, I.,Wiggs, G.F.S., 1995. Analysis of linear sand dune morphological variability, southwestern Kalahari Desert. Geomorphology 11, 189–203.

Bullard, J.E., Thomas, D.S.G., Livingstone, I., Wiggs, G.F.S., 1997. Dune field activity and interactions with climatic variability in the southwest Kalahari Desert. Earth Surface Processes and Landforms 22, 165–174.

Cotes T.F., C.J. Taylor, D.H. Cooper, J. Graham, 1995. Active shape models – their training and application. Computer Vision and Image Understanding (61): 38-59

Cutts, J.A., Smith, R.S.U., 1973. Eolian deposits and dunes on Mars. Journal of Geophysical Research 78, 4139–4154.

Durán, O., Schwämmle, V., Herrmann, H.J., 2005. Breeding and solitary wave behaviour of dunes. Physical Review E 72, 021308. doi:10.1103/PhysRevE.72.021308.

Elbelrhiti, H. and Hargitai H: 2015. Encyclopedia of Planetary Landforms, Chapter: Barchan, p123, Publisher: Springer New York.

Elbelrhiti H, Claudin P and Andreotti B: 2008. Barchan dune corridors: field characterization and investigation of control parameters, J. Geophys. Res., 113, F02S15.

Ewing, R.C., Kocurek, G., Lake, L.W., 2006. Pattern analysis of dune-field parameters. Earth Surface Processes and Landforms 31, 1176–1191.

Ewing, R.C., Peyret, A.-P.B., Kocurek, G., Bourke, M.C., 2010. Dune field pattern formation and recent transporting winds in the Olympia Undae Dune field, north polar region of Mars. Journal of Geophysical Research 115, E08005.

Florensky, C.P., Ronca, L.B., Basilevsky, A.T., 1977. Geomorphic degradations on the surface of Venus: an analysis of Venera 9 and Venera 10 data. Science 196 (4292), 869–871

Hayward, R.K., Mullins, K.F., Fenton, L.K., Hare, T.M., Titus, T.N., Bourke, M.C., Colaprete, A., Christensen, P.R., 2007a. Global Digital Dune Database and initial science results. Journal of Geophysical Research 112, E11007.

Hansen, C.J., Bourke,M.C., Bridges, N.T., Byrne, S., Colon, C., Diniega, S., Dundas, C., Herkenhoff,K., McEwen, A., Mellon, M., Portyankina, G., Thomas, N., 2011. Seasonal erosion and restoration of Mars' Northern Polar Dunes. Science 331, 575–578.

Hersen, P., Andersen, K.H., Elbelrhiti, H., Andreotti, B., Claudin, P., Douady, S., 2004. Corridors of barchan dunes: stability and size selection. Physical Review E 69, 011304. doi:10.1103/PhysRevE.69.011304.

Hersen, P., 2005. Flow effects on the morphology and dynamics of aeolian and subaqueous barchan dunes. Journal of Geophysical Research 110 (F04S07). doi:10.1029/2004JF000185.

Hugenholtz CH, Levin N, Barchyn TE, Baddock M, 2012. Remote sensing and spatial analysis of aeolian sand dunes: a review and outlook. Earth-Science Reviews 111: 319-334

Hugenholtz, C.H., Barchyn, T.E., 2010. Spatial analysis of sand dunes with a new global topographic dataset: new approaches and opportunities. Earth Surface Processes and Landforms 35, 986–992.

Hugenholtz, C.H., Wolfe, S.A., 2005. Recent stabilization of active sand dunes on the Canadian prairies and relation to recent climate variations. Geomorphology 68, 131–147.

Jackson, D.W.T., Beyers, J.H.M., Lynch, K., Cooper, J.A.G., Baas, A.C.W., Delgado-Fernandez, I., 2011. Investigation of three-dimensional wind flow behavior over coastal dune morphology under offshore winds using computational fluid dynamics (CFD) and ultrasonic anemometry. Earth Surface Processes and Landforms 36, 1113–1124.

Jimenez, J.A., Maia, L.P., Serra, J., Morias, J., 1999. Aeolian dune migration along the Ceara coast, north-eastern Brazil. Sedimentology 46, 689–701.

Katsuki, A., Kikuchu, M., Nishimori, H., Endo, N., Taniguchi, K., 2011. Cellular model for sand dunes with saltation, avalanche and strong erosion: collisional simulation of barchans. Earth Surface Processes and Landforms 36, 372–382.

Levin, N., Ben-Dor, E., 2004. Monitoring sand dune stabilization along the coastal dunes of Ashdod-Nizanim, Israel, 1945–1999. Journal of Arid Environments 58, 335–355.

Levin, N., Ben-Dor, E., Karnieli, A., 2004. Topographic information of sand dunes as extracted from shading effects using Landsat images. Remote Sensing of Environment90, 190–209.

Levin, N., Tsoar, H., Herrmann, H.J., Claudino-Sales, V., Maia, L.P., 2009. Modeling the formation of arcuate vegetated dune ridges behind barchan dunes in NE Brazil. Sedimentology 56, 1623–1641.

Liao Shengcai, Xiangxin Zhu, Zhen Lei, Lun Zhang and Stan Z. Li. Learning Multi-scale Block Local Binary Patterns for Face Recognition. International Conference on Biometrics (ICB), 2007, pp. 828-837.

McKee, E.D., 1979. Introduction to a study of global sand seas. In: McKee, E.D. (Ed.), A Study of Global Sand Seas: United States Geological Survey, Professional Paper, 1052, pp. 3–19.

Necsoiu, M., Leprince, S., Hooper, D.M., Dinwiddie, C.L., McGinnis, R.N., Walter, G.R., 2009. Monitoring migration rates of an active subarctic dune field using optical imagery. Remote Sensing of Environment 113, 2441–2447.

Nield, J.M., Baas, A.C.W., 2008. The influence of different environmental and climatic conditions on vegetated aeolian dune landscape development and response. Global and Planetary Change 64, 76–92.

Okin, G.S., 2008. A new model of wind erosion in the presence of vegetation. Journal of Geophysical Research 113 (F02S10). doi:10.1029/2007JF000758.

Paul Viola, Michael J. Jones. Rapid Object Detection using a Boosted Cascade of Simple Features. Conference on Computer Vision and Pattern Recognition (CVPR), 2001, pp. 511-518

Pinker, R.T., Karnieli, A., 1995. Characteristic spectral reflectance characteristics of a semi-arid environment. International Journal of Remote Sensing 16, 1341–1363.

Reitz, M.D., Jerolmack, D.J., Ewing, R.C., Martin, R.L., 2010. Barchan-parabolic dune pattern transition from vegetation stability threshold. Geophysical Research Letters 37, L19402.

Schatz, V., Tsoar, H., Edgett, K.S., Parteli, E.J.R., Herrmann, H.J., 2006. Evidence for indurated sand dunes in the Martian north polar region. Journal of Geophysical Research 111, E04006.

Scheidt, S., Ramsey, M., Lancaster, N., 2010. Determining soil moisture and sediment availability at White Sands Dune field, New Mexico, from apparent thermal inertia data. Journal of Geophysical Research 115, F02019.

Silvestro, S., Fenton, L.K., Vaz, D.A., Bridges, N.T., Ori, G.G., 2010. Ripple migration and dune activity on Mars: evidence for dynamic wind processes. Geophysical Research Letters 37, L20203.

Til, M., van Bijlmer, A., de Lange, R., 2004. Seasonal variability in spectral reflectance of coastal dune vegetation. EASReL eProceedings 3 (2/2004), 154–165.

Tsoar, H., Karnieli, A., 1996. What determines the spectral reflectance of the Negev–Sinai sand dunes. International Journal of Remote Sensing 17, 513–525.

Tsoar, H., 2001. Types of Aeolian Sand Dunes and Their Formation. Geomorphological Fluid Mechanics. N.J. Balmforth and A. Provenzale (Eds.): LNP 582, pp. 403–429, 2001. c Springer-Verlag Berlin Heidelberg

Tsoar, H., 2005. Sand dunes mobility and stability in relation to climate. Physica A 357, 50–56.

Vermeesch, P., Drake, N., 2008. Remotely sensed dune celerity and sand flux measurements of the world's fastest barchans (Bodélé, Chad). Geophysical Research Letters 35, L24404.

Wasson, R.J., Hyde, R., 1983. Factors determining desert dune type. Nature 304, 337–339.

Wilkins, D.E., Ford, R.L., 2007. Nearest neighbor methods applied to dune field organization: the Coral Pink Sand Dunes, Kane County, Utah, USA. Geomorphology 83, 48–57.

Wolfe, S.A., Huntley, D., Ollerhead, J., 2004. Relict Late Wisconsinan dune fields of the northern Great Plains, Canada. Géographie Physique et Quaternaire 58, 323–336.

Wolfe, S.A., Hugenholtz, C.H., 2009. Barchan dunes stabilized under recent climate warming on the northern Great Plains. Geology 37, 1039–1042.